



A Pin-on-Disk Tribometer for Friction and Lubricating Performance in mm-Scale

Jian Wu^{1,3} · Tonggang Liu² · Ning Yu¹ · Jiejie Cao¹ · Kesheng Wang³ · Knut Sørby³

Received: 25 June 2020 / Accepted: 5 February 2021 / Published online: 21 February 2021
© The Author(s), under exclusive licence to Springer Science+Business Media, LLC part of Springer Nature 2021

Abstract

A pin-on-disk tribometer for micro-scale applications is presented in this paper. The tribometer consists of a stationary mm-scale pin and a rotating disk. Friction and lubrication film thickness are measured by a laser position detector and a laser displacement sensor. Using this tribometer, hydrodynamic tests have been carried out with the specimens fully submerged in a lubricant. Results suggest that the sliding motion in the mm-scale operates with a direct contact at low speed, and in the hydrodynamic regime at a higher speed. When the sliding reaches the critical speed, the lubricant film is established, and the thickness of the film stabilizes and the friction increases with the sliding speed. The tribometer shows good repeatability in these tests.

Keywords MEMS devices · Friction test methods · Boundary lubrication · Hydrodynamic lubrication

1 Introduction

The size of a Micro-Electronic-Mechanical-System (MEMS) is usually on the mesoscopic scale (0.1 μm ~ 1 mm). The characteristics of moving micro-parts (such as micro-motor and micro-switches) are affected by both surface and volume forces, which is different from the situation on the macro scale. The wear due to the large surface area to volume ratio restricts the development of MEMS. In order to reduce friction in MEMS, various methods have been applied, such as surface treatment [1], organic monolayers [2], dry coating [3, 4], vapor phase [5], and liquid lubrication [6, 7].

A large number of experimental methods have been employed to study friction between micro-scale surfaces. The most common method is atomic force microscopy (AFM) [8] and the friction force microscope (FFM). In

addition, several examples of MEMS tribometers have been developed. Gatzen et al. [9] used a pin-on-disk tester to study the effect of surface roughness on wear for a silicon-on-silicon micro-contact, and they showed that the largest wear was produced by a surface with high initial roughness. Beerschwinger et al. [10] built a MEMS tribometer to study the effect of surface topography on wear in MEMS devices. They found that the wear rates are either dominated by asperity fracture or asperity deformation. Patton et al. [11] designed an advanced ball-on-disk test rig to study MEMS materials, which can measure friction, electrical contact resistance, wafer surface reflectance, and other properties. Bandorf et al. [12] used a pin-on-disk set-up to investigate friction and wear of various diamond-like coatings deposited on substrates of varying hardness. It was found that the friction coefficient was load-dependent at the microscopic scale, and friction was greatly reduced when a substrate of high elastic modulus was used. Ku et al. [13, 14] developed a flat-on-flat tribometer to investigate suitable methods for lubricating in MEMS. It proved that lubrication by fluids or vapors were effective in MEMS.

This paper presents a pin-on-disk tribometer which can be used to measure friction and the lubrication film thickness in the mm-scale. The principle of the tribometer and laser measurement systems is described. Using this tribometer, the friction and lubricant performance have been tested, and the repeatability of the system has been studied.

✉ Jian Wu
wujian@cslg.edu.cn

¹ College of Mechanical and Electrical Engineering, Changshu Institute of Technology, Changshu 215500, China

² College of Mechanical and Electrical Engineering, China University of Mining and Technology, Xuzhou 221116, China

³ Department of Mechanical and Industrial Engineering, Norwegian University of Science and Technology, 7491 Trondheim, Norway

2 Design of the Tribometer

2.1 The Principle of Measurement System

The assembly of the tribometer in this study is shown in Fig. 1. It contains a 5-axis adjustable fixture (Thorlabs, MBT 501) for positioning and orientation of the test specimen and a vertically adjustable device for the rotating disk. A planar torsional spring and the planar normal spring are installed at each end of a support arm. The planar torsional spring is mounted on the 5-axis fixture. The mm-scale specimen is installed under the planar normal spring, as shown in Fig. 2. In the test, the vertical position of the rotation disk is adjusted until the disk contacts the specimen surface. The applied normal force can be obtained by measuring the deflection of the planar normal spring. For the horizontal measurement, a laser beam is deflected through the triangular prism and then directed into the position detector. The friction force on the test specimen rotates the support arm around the plane torsional spring, and the laser spot will move on the detector surface.

The normal force between the pin specimen and the rotating disk is applied by adjusting the vertical position of

the disk. When there is contact between the specimen and the disk, the planar normal spring is deformed as shown in Fig. 3. The applied force is obtained by Eq. (1). Where N is the applied force on pin and disk surface (N), k_1 is the stiffness of planar normal spring (N/m), and Δx is the displacement measured by the laser displacement sensor, (Keyence, G30).

$$N = k_1 \Delta x \tag{1}$$

The principle of the laser-based measurement system used in this work as shown in Fig. 4. When a friction force, f , is acting on the specimen surface, the planar torsional spring will rotate a small angle α , and a laser spot reflected by a triangular prism is shifted by ΔL on the position detector (Thorlabs, PDP90A), the details can be readied in reference [15].

The friction can be written as:

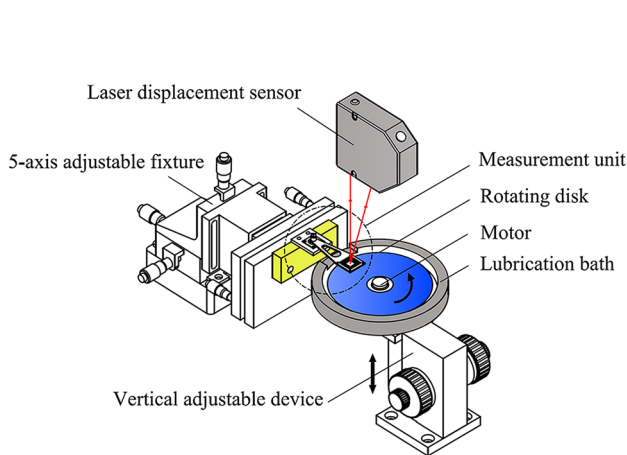


Fig. 1 The assembly drawing of the tribometer

Fig. 2 Details of the measurement unit

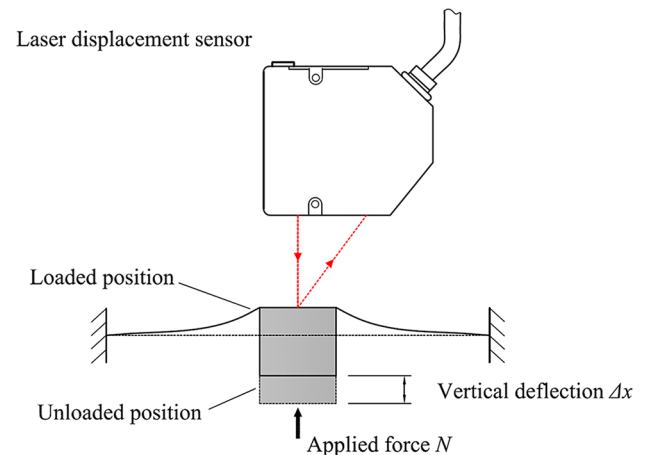
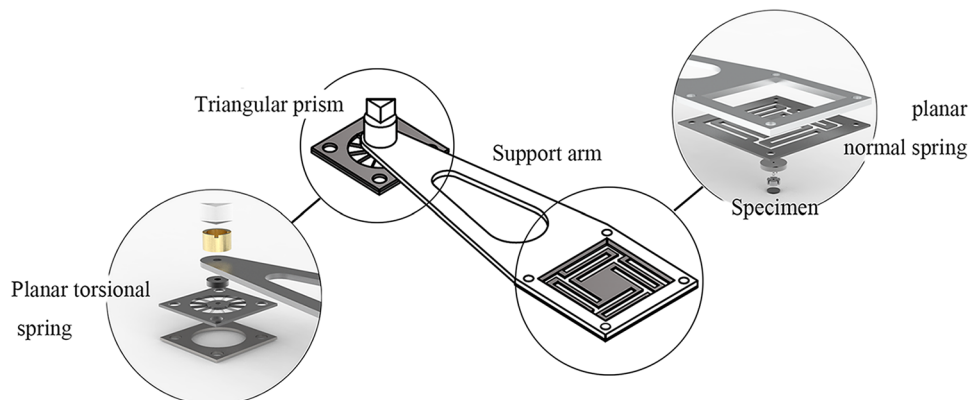


Fig. 3 Illustration of the normal applied force

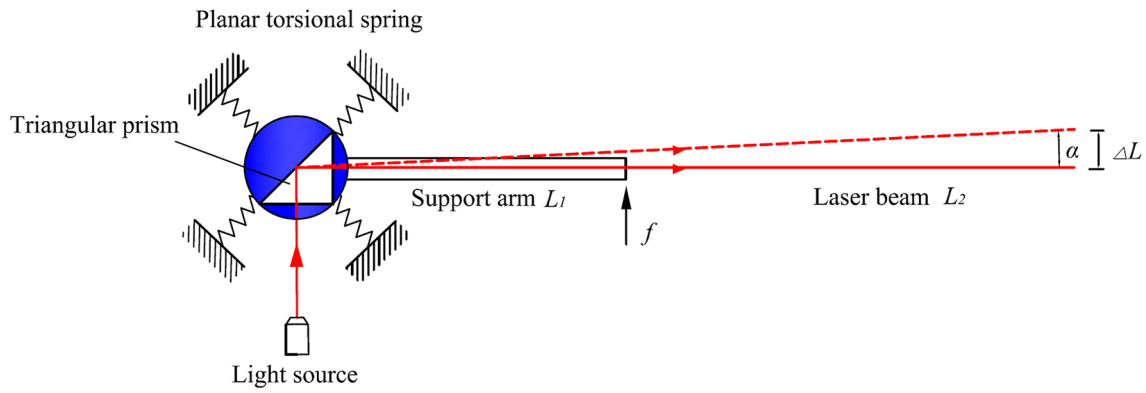


Fig. 4 The principle of measurement for friction

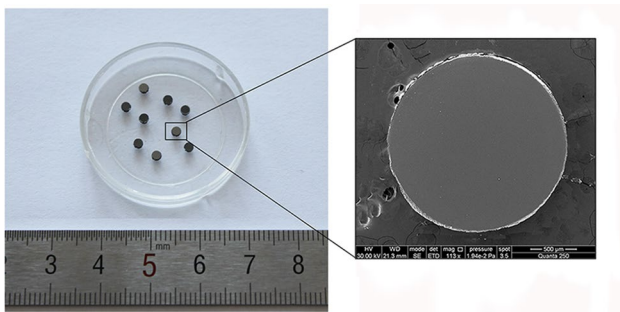


Fig. 5 Photo and SEM of pin specimen

$$f \approx k_2 \frac{\Delta L}{L_1 L_2} \tag{2}$$

where k_2 is the stiffness of the planar torsional spring (Nm/rad), ΔL is the shift of the laser spot (m), L_1 is the length of the support arm (m), and L_2 is the length of the laser path (m).

2.2 Pin Specimen and Rotating Disk

The specimen used in the experiments is made of Si (100), Young’s modulus (E) of the material is 168 GPa, the Poisson’s ratio (γ) is 0.28, and the material density (ρ) is $2.33 \times 10^3 \text{ kg/m}^3$. The diameter of the specimen is 2 mm, and the thickness is 0.3 mm, as shown in Fig. 5. Figure 6 shows the rotating disk, which consists of a 0.5-mm thick silicon disk (Si (100)) that is attached to a rigid support disk. Both the specimen and the rotating disk are prepared by laser processing.

2.3 Lubrication Mechanism

In order to test the friction of micro-specimens under liquid lubrication, a lubrication bath with a pumping system was designed as shown in Fig. 7. The lubricant is applied to the

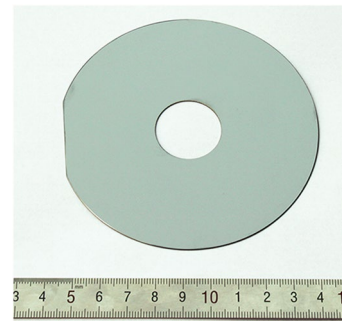


Fig. 6 Photo of a disk specimen

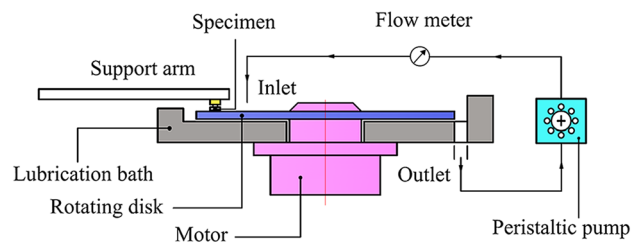


Fig. 7 Schematic diagram of liquid lubrication set up

surface of the rotating disk and flow to the test specimen by centrifugal force, which ensures the friction pair is completely wetted by lubricants during the test. The lubrication used in the test is hexadecane, which was selected for its low viscosity (3.03 mPa·s, 25 °C).

3 Testing

3.1 The Parameters of Measurement

All components of the tribometer are fixed on a 600 × 600 mm optical plate, as illustrated in Fig. 8a. The

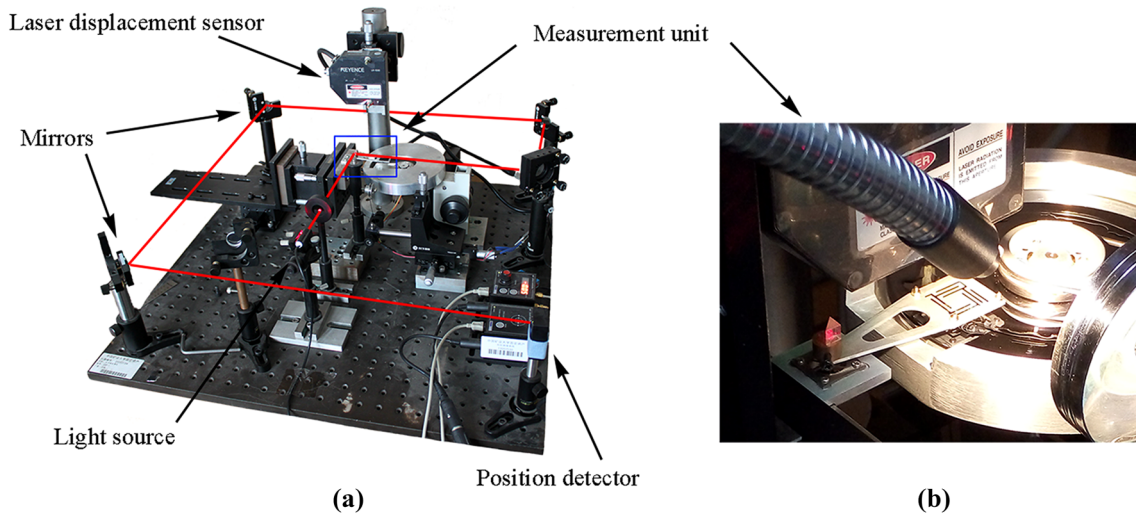


Fig. 8 Photographs of the tribometer. **a** The photo of the test rig, with the path of light highlighted in red. **b** The photo of the measurement process

Table 1 The parameters of the tribometer

No	Name	Range	Resolution
1	The normal load, N	0–0.2 N	78.8 μN
2	The friction force, f	± 150 mN	53.1 μN
3	Speed	10 – 600 rpm	1 rpm
4	Wear track diameter	45 – 90 mm	0.02 mm
5	Film thickness	0 – 1 mm	0.01 μm

Table 2 Specific working conditions and measurement errors

Input variable	Base value	Input error	Error of friction coefficient (%)
L_1	50 mm	50–0.0005 mm	0.001%
L_2	2100 mm	2100+0.021 mm	0.001%
ΔL_{max}	0.214 mm	0.214+0.016 mm	7.5%
Δx_{max}	9.6 μm	9.6+1.2 μm	12.5%

length of the support arm $L_1 = 50$ mm, and the length of the laser path $L_2 = 2.1$ m. The stiffness of the planar normal spring and the planar torsional spring is calibrated before testing ($k_1 = 7880$ N/m, $k_2 = 7.44$ Nm/rad). Then, the friction coefficient can be written as:

$$\mu = \frac{f}{N} = \frac{T}{L_1 k_1 \Delta x} \approx \frac{k_2 \Delta L}{k_1 L_1 L_2 \Delta x} = 8.99 \times 10^{-3} \frac{\Delta L}{\Delta x} \quad (3)$$

In this test rig, the laser displacement sensor has a resolution of 0.01 μm and a measurement range of ± 3 mm. The position detector has an accuracy of 0.75 μm and a range of ± 4.5 mm. Consider the noise, drift and alignment, the parameters of the tribometer are listed in Table 1. Figure 8b shows an image of the measurement process.

In the test, the normal force is applied by adjusting the vertical position of the disk before the motor that rotates the disk is started. The laser displacement sensor and the position detector are used to measure the friction force, f , and film thickness, (Δx), respectively. In each test, the sliding speed is kept constant for some seconds to get a stable average measurement of the normal force and friction

force. All experiments have been done at room temperature 20–25 $^\circ\text{C}$.

3.2 The Error of Measurement

The error of measurement comes from the prolong of the length of the support arm L_1 and the length of the laser path L_2 , the shift of the laser spot ΔL , and the displacement measured by the laser displacement sensor Δx . The error of three parameters to the measurement system as shown in Table 2.

4 Results and Discussion

4.1 Friction and Film Thickness

Using the measurement system, friction and lubricating performance have been studied in the following experiments. An initial force (0.16 N) has been applied between the pin and disk before starting the rotation of the disk. Then, the friction and the film thickness have been obtained by the position detector and the laser displacement sensor, respectively. During the test, hexadecane is supplied by the pump.

Figure 9 shows how the measured friction coefficient varies with sliding speed. To show the friction at a low speed more clearly, a logarithmic scale is used on the abscissa. It can be seen that the friction curve has three regions, similar to the Stribeck curve. When the sliding is low, the friction coefficient is high (0.13–0.18). As seen from the graph, there is some scattering of the results. When the sliding speed increases to a certain value (~ 0.05 m/s), the friction decreases sharply. When the speed is increased further the friction increases slightly. At the higher speed, the results are less scattered.

The vertical position of the planar normal spring is monitored throughout the tests, and this can be used to measure the film thickness. Measurements of the film thickness are shown in Fig. 10. At low speed, the film thickness between the contact surfaces is not stable, and it varies between 0 and 5 μm . When the speed reaches 0.05 m/s, the lubrication fluid enters the contact surface and forms a film with a certain thickness. At the higher speed, the lubrication film is stable, and it increases slightly as the sliding speed increases. In this test, the film thickness is below 10 μm .

At low sliding speed, the surfaces are in direct contact with each other, and no effective lubricating film is formed. The lubrication film is not stable, and there is some scattering of the measurements of both friction coefficient and film thickness. When the sliding speed reaches a certain value, the lubrication fluid enters the contact surfaces and forms a lubricating film. When the sliding speed is increased further, the pressure between the surfaces increases, and the load capacity of the fluid film increases. The gap between the surfaces is increased, balanced by the planar normal spring. At higher sliding speeds, the friction increases slightly with the increased shearing of the fluid.

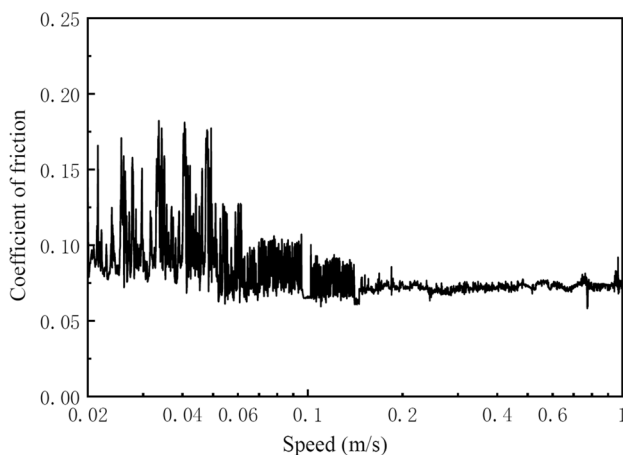


Fig. 9 Friction measured by the system

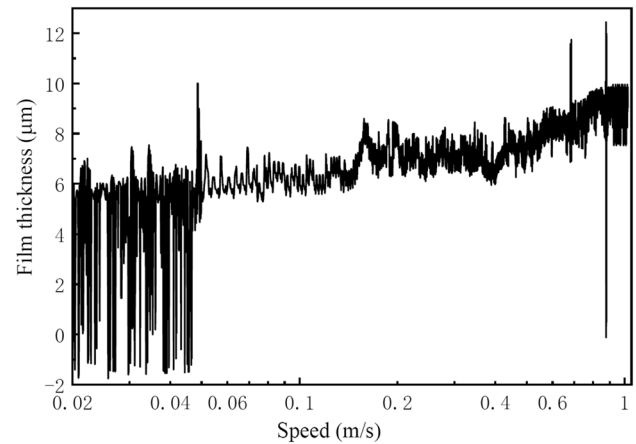


Fig. 10 Film thickness measured by the system

4.2 Repeatability

The tests shown in the previous sections were repeated two times under similar conditions. The coefficient of friction at a certain speed is used on average in three measurements. To ensure independent results, the test specimen was taken out and then reinstalled and reloaded again. Figure 11 shows the results of all three measurements.

It can be seen from the experimental results that there is a similar trend in all three tests. The friction coefficient is relatively high at low speed. There is some scattering of the results, probably due to the random nature of the stick–slip effect. In the range 0.01–0.05 m/s the friction was measured at 56 different speeds. The pooled repeatability standard deviation for these friction coefficient measurements is 0.016. The difference between the highest and lowest friction coefficient measurement at one single speed is 0.112. When the sliding speed increases to a certain value, the friction decreases sharply. In the three measurements, the speed

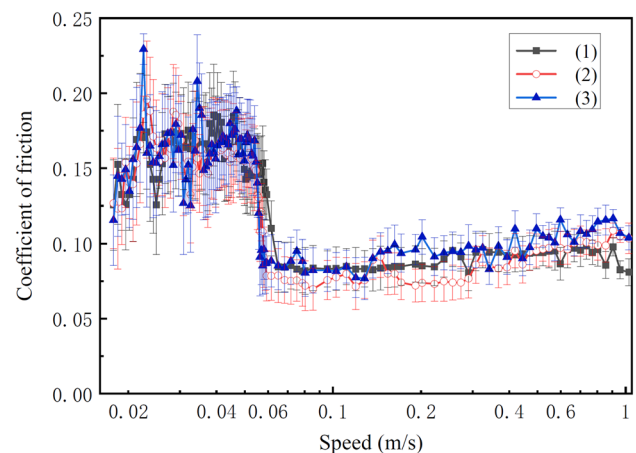


Fig. 11 Three friction coefficient measurements

at which the friction began to decrease was 0.059 m/s, 0.055 m/s, and 0.055 m/s. When the speed is increased further, the friction increases slightly in all three measurements. At sliding speed above 0.12 m/s, the friction coefficient differs slightly between the tests. The greater the sliding speed, the more obvious the difference. A possible explanation for the variation is that the specimens are installed with slightly different angles to the disk, which could give variations in the fluid pressure distribution on the surface. This effect is particularly evident for specimens in mm-scale. The pooled repeatability standard deviation in the range of 0.06–1.0 m/s is 0.0143. The difference between the highest and lowest friction coefficient measurement at one single speed is 0.04.

5 Conclusions

A new tribometer has been developed to measure the friction of the mm-scale. This device is capable of studying the friction and lubrication performance of microscale under different sliding speeds. A pin-on-disk contact has been used to simulate the mm-scale contact. Laser techniques were used to measure the applied normal force and friction. A series of experiments were carried out using this system. The results suggest that the measurement system has good repeatability for micro force measurements, and the use of lubricants in the mm-scale still operates in the hydrodynamic regime. Future research will focus on the lubrication performance of the sub-mm-scale surface.

Acknowledgements The work is supported by the National Natural Science Foundation of China (No. 61803048), Jiangsu Government Scholarship for Overseas Studies, Open Project of Jiangsu Elevator Intelligent Safety Key Construction Laboratory (JSKLESS201703), and The Doctoral Science Foundation of Changshu Institute of Technology (No. KYZ2015054Z).

Compliance with Ethical Standards

Conflict of interest The authors declare no competing interest.

References

1. Tayebi, N., Polycarpou, A.A.: Reducing the effects of adhesion and friction in microelectromechanical systems (MEMSs) through surface roughening: comparison between theory and experiments. *J. Appl. Phys.* **98**, 073528 (2005). <https://doi.org/10.1063/1.2058178>
2. Ashurst, W.R., Yau, C., Carraro, C., Lee, C., Kluth, G.J., Howe, R.T., Maboudian, R.: Alkene based monolayer films as

- anti-stiction coatings for polysilicon MEMS. *Sensors Actuators, A Phys.* **91**, 239–248 (2001). [https://doi.org/10.1016/S0924-4247\(01\)00593-3](https://doi.org/10.1016/S0924-4247(01)00593-3)
3. Luo, J.K., Fu, Y.Q., Le, H.R., Williams, J.A., Spearing, S.M., Milne, W.I.: Diamond and diamond-like carbon MEMS. *J. Micro-mechanics Microengineering.* **17**, S147–S163 (2007). <https://doi.org/10.1088/0960-1317/17/7/S12>
4. Le, H.R., Williams, J.A., Luo, J.K.: Characterisation of tribological behaviour of silicon and ceramic coatings under repeated sliding at micro-scale. *Int. J. Surf. Sci. Eng.* **2**, 1–13 (2008). <https://doi.org/10.1504/IJSURFSE.2008.018964>
5. Neeyakorn, W., Varma, M., Jaye, C., Burnette, J.E., Lee, S.M., Nemanich, R.J., Grant, C.S., Krim, J.: Dynamics of vapor-phase organophosphates on silicon and OTS. *Tribol. Lett.* **27**, 269–276 (2007). <https://doi.org/10.1007/s11249-007-9224-y>
6. Reddyhoff, T., Ku, I.S.Y., Holmes, A.S., Spikes, H.A.: Friction modifier behaviour in lubricated MEMS devices. *Tribol. Lett.* **41**, 239–246 (2011). <https://doi.org/10.1007/s11249-010-9704-3>
7. Zhao, W., Zhu, M., Mo, Y., Bai, M.: Effect of anion on micro/nano-tribological properties of ultra-thin imidazolium ionic liquid films on silicon wafer. *Colloids Surfaces A Physicochem. Eng. Asp.* **332**, 78–83 (2009). <https://doi.org/10.1016/j.colsurf.2008.09.025>
8. Bhushan, B., Kasai, T., Kulik, G., Barbieri, L., Hoffmann, P.: AFM study of perfluoroalkylsilane and alkylsilane self-assembled monolayers for anti-stiction in MEMS/NEMS. *Ultramicroscopy* **105**, 176–188 (2005). <https://doi.org/10.1016/j.ultra.2005.06.034>
9. Gatzert, H.H., Beck, M.: Tribological investigations on micromachined silicon sliders. *Tribol. Int.* **36**, 279–283 (2003). [https://doi.org/10.1016/S0301-679X\(02\)00198-6](https://doi.org/10.1016/S0301-679X(02)00198-6)
10. Beerschwinger, U., Mathieson, D., Reuben, R.L., Yang, S.J.: A study of wear on mems contact morphologies. *J. Micro-mechanics Microengineering.* **4**, 95–105 (1994). <https://doi.org/10.1088/0960-1317/4/3/001>
11. Patton, S.T., Zabinski, J.S.: Advanced tribometer for in situ studies of friction, wear, and contact condition - advanced tribometer for friction and wear studies. *Tribol. Lett.* **13**, 263–273 (2002). <https://doi.org/10.1023/A:1021063326225>
12. Bandorf, R., Lüthje, H., Staedler, T.: Influencing factors on micro-tribology of DLC films for MEMS and microactuators. *Diam. Relat. Mater.* **13**, 1491–1493 (2004). <https://doi.org/10.1016/j.diamond.2004.01.032>
13. Ku, I.S.Y., Reddyhoff, T., Choo, J.H., Holmes, A.S., Spikes, H.A.: A novel tribometer for the measurement of friction in MEMS. *Tribol. Int.* **43**, 1087–1090 (2010). <https://doi.org/10.1016/j.triboint.2009.12.029>
14. Ku, I.S.Y., Reddyhoff, T., Holmes, A.S., Spikes, H.A.: Wear of silicon surfaces in MEMS. *Wear* **271**, 1050–1058 (2011). <https://doi.org/10.1016/j.wear.2011.04.005>
15. Wu, J., Liu, T., Wang, K., Sørby, K.: A measuring method for micro force based on MEMS planar torsional spring. *Meas. Sci. Technol.* (2020). <https://doi.org/10.1088/1361-6501/ab9acd>

Publisher's Note Springer Nature remains neutral with regard to jurisdictional claims in published maps and institutional affiliations.